

Critical behavior in the half-metallic Heusler alloy Co₂TiSnAzizur Rahman,¹ Majeed ur Rehman,¹ Dechen Zhang,¹ Min Zhang,¹ Xiangqi Wang,¹ Rucheng Dai,² Zhongping Wang,² Xiaoping Tao,² Lei Zhang³,⁴ and Zengming Zhang^{2,4,*}¹*Department of Physics, University of Science and Technology of China, Hefei 230026, China*²*The Centre for Physical Experiments, University of Science and Technology of China, Hefei 230026, China*³*High Magnetic Field Laboratory, Chinese Academy of Sciences, Hefei 230031, China*⁴*Key Laboratory of Strongly-Coupled Quantum Matter Physics, Chinese Academy of Sciences, School of Physical Sciences, University of Science and Technology of China, Hefei, Anhui 230026, China*

(Received 22 September 2019; revised manuscript received 12 November 2019; published 16 December 2019)

The critical behavior of Heusler alloy Co₂TiSn is investigated by bulk magnetization study around the paramagnetic to ferromagnetic transition. The precise value of Curie temperature ($T_c = 358$ K) as well as the critical exponents ($\beta = 0.527 \pm 0.003$, $\gamma = 1.229 \pm 0.002$, and $\delta = 3.33 \pm 0.002$) were determined by means of different analytical methods such as modified Arrott plot analysis, the Kouvel-Fisher method, and critical isotherm analysis. With these critical exponents the isotherm $M(H)$ curves below and above T_c collapse into two universal branches, fulfilling the single scaling equation $m = f_{\pm}h$, where m and h are normalized magnetization and field, respectively. The reliability of the critical exponents were confirmed by Widom scaling hypothesis $\delta = \gamma\beta^{-1}$. Apart from the slight increase in β and γ , the deduced critical exponents were consistent with the theoretical prediction of the mean-field model, indicating the long range magnetic interaction in Co₂TiSn. Additionally, it is obtained that spin interaction decays as $J(r) \sim r^{-4.7}$. We suggest that the competition between localized majority spins and itinerant minority spins magnetic interaction could be responsible for critical behavior in Co₂TiSn.

DOI: [10.1103/PhysRevB.100.214419](https://doi.org/10.1103/PhysRevB.100.214419)**I. INTRODUCTION**

Heusler alloys, which are also known as full-Heusler alloys to distinguish from half-Heusler alloys, are generally described as intermetallic ternary compounds designed in the stoichiometric composition X_2YZ , where X and Y represent transition elements and Z is an sp element, whereas half-Heusler alloys are crystallized in the XYZ stoichiometric composition. Heusler alloys have drawn considerable attention due to owning high Curie temperature and easy tunable electronic, structural, or magnetic properties [1–5]. Co-based Heusler alloys host some additional properties of so-called half-metallicity with full spin polarization at the Fermi level [4,6,7], which is very demandable for spintronics applications [8,9]. Several Co-based Heusler alloys such as Co₂MnSi, Co₂MnGe, Co₂FeAl_{0.5}Si_{0.5}, and Co₂TiX ($X = \text{Si, Ge, or Sn}$) have been predicted to be half-metal [7,10–14] with Weyl points at the Fermi surface [15,16].

Co-based Heusler alloys are supposed to be high-grade candidates for examining itinerant electron ferromagnetism. Of these, the Co₂TiSn compound is of notable importance because of its similarity with the prototype half-metallic system NiMnSb, which is a potential spin-injector material for spintronics applications [17]. Co₂TiSn exists in a half-metallic ferromagnetic state with a magnetic moment of $2\mu_B$ and a Curie temperature T_c around 355 K [4,18,19]. Anomalous negative magnetoresistance above T_c up to nearly 370 K

and a negative magnetoresistance peak in the vicinity of T_c reveal that electrical resistivity is strongly linked with the magnetic behavior in the Co₂TiSn compound [20]. This indicates that there exists the large spin fluctuations near paramagnetic to ferromagnetic (PM-FM) transition in this material as an itinerant electron system [18]. A number of studies from the viewpoint of spin fluctuations near T_c focused on the electric properties [20,21] and the pressure dependent magnetic properties [18] for Co₂TiSn. In addition to this, recently first principles studies on Co₂TiSn revealed its other interesting characteristics. For instance, Chang *et al.* [22] identified a topological semimetallic state in FM phase Co₂TiSn and further revealed the presence of Weyl nodes by the inclusion of spin orbit coupling. Ernst *et al.* [23] showed the existence of intrinsic anomalous Hall conductivity in Co₂TiSn, originated from slightly gapped nodal lines due to symmetry reduction induced by magnetization. The Heusler compound Co₂TiSn has been studied extensively both theoretically and experimentally. However, more investigations are required to explore its intrinsic magnetic interactions. As reported previously [24–26], analysis of the critical exponent in the vicinity of the PM-FM transition region is an effective method for clarifying magnetic interactions and properties.

In this work, we study the critical behavior of the half-metallic Heusler alloy Co₂TiSn. The nature of FM transition and its magnetic mechanism in the critical region is found to be mean field like, except that β and γ are slightly larger than theoretical values.

*Corresponding author: zzm@ustc.edu.cn

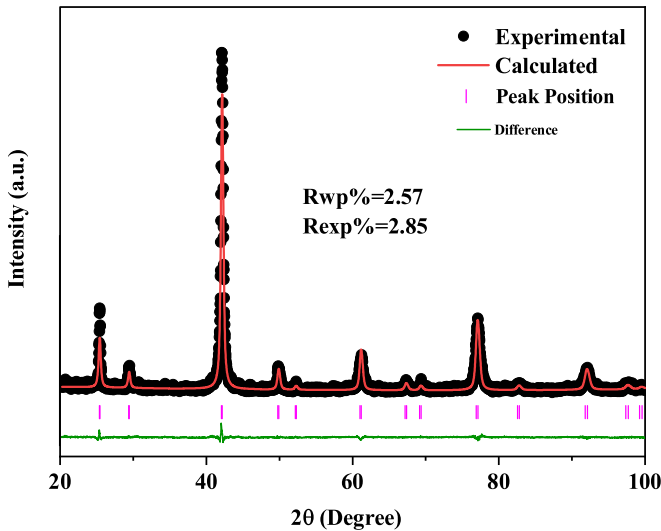


FIG. 1. (a) Refined powder XRD pattern of Co_2TiSn at room temperature. The black solid spheres represent the experimental data and the solid red line is the calculated result. The solid green line at the bottom corresponds to the difference between the experimental and fitted intensities.

II. METHODS

An ordered Heusler alloy Co_2TiSn was synthesized via repeated melting of the stoichiometric composed mixtures of 99.9% pure Ti, 99.9% pure Co, and 99.999% pure Sn in an argon arc furnace. A reaction product was sealed in a quartz tube together with an appropriate quantity of argon gas for heat treatment to achieve a homogenized sample, sustained at 1100°C for 3 days and then quenched in water. The structure and phase purity of the Co_2TiSn were characterized by x-ray diffraction (XRD) (Rigaku SmartLab) with $\text{Cu } K\alpha$ radiation. The magnetization of the samples was measured by SQUID-VSM (Quantum Design, USA). The sample was processed to form an ellipsoid and to reduce the demagnetizing field the magnetic field was applied along the longest semiaxis. To ensure that each curve was initially magnetized, isothermal magnetization was performed after long enough heating of the sample well above T_c , then cooled to the desired temperature under zero field. The applied magnetic field H_a was adjusted into an internal field as $H_i = H_a - NM$ (where N is the demagnetization variable and M is the measured magnetization acquired as in [27]). The calculated H_i was used for critical behavior analysis.

III. RESULTS AND DISCUSSION

A Heusler alloy (X_2YZ) that crystallizes in the $L2_1$ structure with four interpenetrating face centered cubic (fcc) sublattices is fully ordered and gives a nonzero structure factor for Bragg reflection when all indices are either odd or even [28]. In the $L2_1$ structure with a space group $Fm\bar{3}m$, Co atoms occupy $A(0, 0, 0)$ and $C(1/2, 1/2, 1/2)$ sites and Ti and Sn atoms occupy $B(1/4, 1/4, 1/4)$ and $D(3/4, 3/4, 3/4)$ sites, respectively. Figure 1 shows room temperature XRD powder diffraction data of Co_2TiSn . Materials analysis using diffraction (MAUD) was employed to refine XRD data. The details

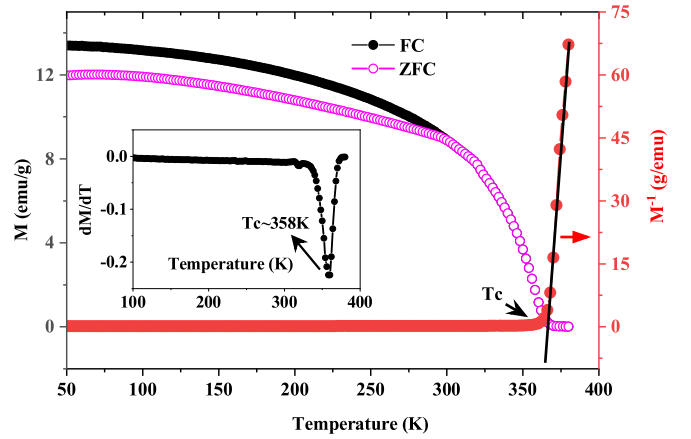


FIG. 2. Temperature dependence of magnetization $M(T)$ on the left and $M^{-1}(T)$ on the right. The inset shows dM/dT vs T (down left).

about XRD refinement can be found elsewhere. The obtained fitting parameters $R_{wp} = 2.57\%$ and $R_{exp} = 2.85\%$ with GOF approaching 1 indicate a Co_2TiSn Heusler alloy displays an almost ideal degree of order as the $L2_1$ phase within the XRD measurement resolution limits. This is very essential to realize the half-metallicity of Co_2TiSn since crystal disorder such as $D0_3$ -type, $B2$ -type, or $A2$ -type usually inhibits Heusler alloys spin polarization [29]. The value of the lattice parameter for synthesized Co_2TiSn samples from the powder XRD patterns was determined to be $6.0573(5) \text{ \AA}$, an agreement with the earlier reported work [10,30,31].

Figure 2 displays the temperature dependence of magnetization $M(T)$ and inverse magnetization $M^{-1}(T)$ for Co_2TiSn under the applied field of 100 Oe. Branching of ZFC and FC in the $M(T)$ curve may be due to the presence of magnetic disorders induced by atomic disorders. A phase transition from PM to FM occurs at $T_c \sim 358 \text{ K}$, estimated from the dM/dT curve (shown in inset of Fig. 2), in agreement with earlier reported work. The $M^{-1}(T)$ deviation from the straight line above T_c shows the occurrence of critical fluctuations even in the PM phase.

Figure 3(a) presents initial isothermal magnetization curves in the critical region around T_c with a temperature interval of 1 K. Generally the critical exponents and the accurate value of T_c can be determined by plotting M^2 versus H/M according to Arrott plot analysis in the critical region [32].

Figure 3(b) shows the Arrott plot with a series of parallel lines. T_c around 358 K is determined from the line through the origin. Moreover, Banerjee's criterion [33] suggests that the nature of the transition could be confirmed by the sign of the slope of these lines, negative for first order and positive for second order. Figure 3(b) displays all the curves forming quasistraight lines, indicating that the magnetic mechanism in Co_2TiSn is mean field like in the critical region. Obviously, the positive slopes of these lines reveal the nature of FM transition is second order. However, these lines are not very straight and no line passed through the origin, indicating that the critical exponents under the framework of the Landau mean-field model, i.e., $\beta = 0.5$ and $\gamma = 1$, need to be modified in order to find the precise value of T_c .

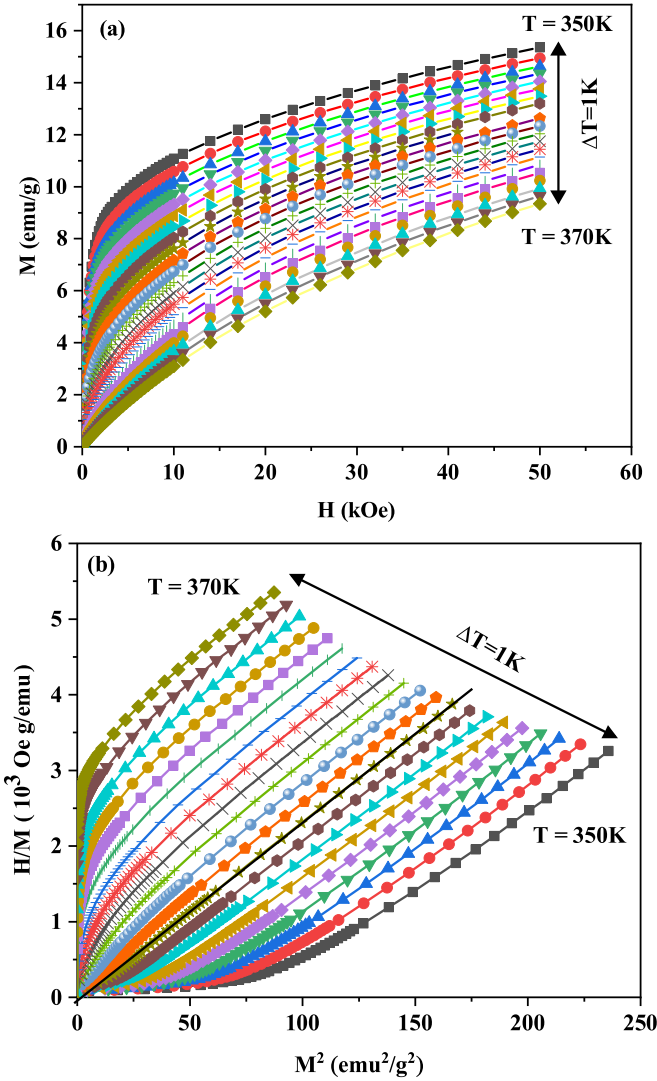


FIG. 3. (a) Initial isothermal magnetization around T_c ; (b) Arrott plot of H/M vs M^2 .

It is widely known that the critical behavior for the second order phase transition can be studied in detail with the help of an interrelated set of critical exponents. In the vicinity of T_c , for second order phase transition, the divergence correlation length $\xi = \xi_0 |(T_c - T)/T_c|^{-\nu}$ leads to the universal scaling laws for the initial magnetic susceptibility χ_0 and spontaneous magnetization (M_S). In this sense, the mathematical relationship of the exponents β [associated with the spontaneous magnetization $M(H = 0)$ below T_c], γ (related to the initial susceptibility above T_c), and δ (related to the critical magnetization at T_c) from the magnetization are given as [34,35]

$$M_S(T) = M_0(-\epsilon)^\beta, \quad \epsilon < 0, \quad (1)$$

$$\chi_0^{-1}(T) = (h_0/M_0)(\epsilon)^\gamma, \quad \epsilon > 0, \quad (2)$$

$$M = DH^{1/\delta}, \quad \epsilon = 0, \quad T = T_c, \quad (3)$$

where $\epsilon = (T - T_c)/T_c$ is the reduced temperature and h_0/M_0 and D are critical amplitudes. Figure 4(a) is generated using the M_S and χ_0^{-1} values obtained by the linear extrapolation from the high field region to the intercepts. Fit-

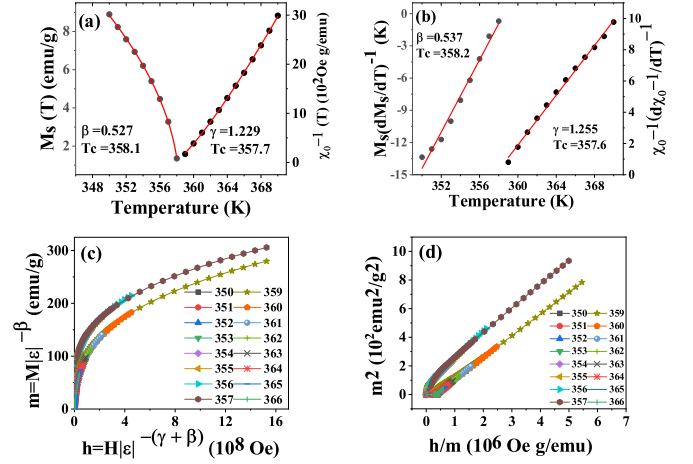


FIG. 4. (a) Spontaneous magnetization M_S (left) and inverse initial susceptibility χ_0^{-1} (right) vs T with the fitting solid curves, (b) KF plots for $M_S(T)$ (left) and $\chi_0^{-1}(T)$ (right) (solid lines are fitted), (c) scaling plots around T_c using β and γ determined by the KF method, and (d) the renormalized magnetization and field plotted as m^2 vs h/m .

ting Eq. (1) and Eq. (2), it is obtained from the modified Arrott plot analysis that $\beta = 0.527 \pm 0.003$ with $T_c = 358.1 \pm 0.2$ and $\gamma = 1.229 \pm 0.002$ with $T_c = 357.7 \pm 0.2$ K. One can clearly observe that the value of T_c obtained using Arrott plot analysis is consistent with that obtained from the $M(T)$ curve.

Alternatively, the critical exponents can be precisely obtained by the Kouvel-Fisher method using Eqs. (4) and (5) [36]. The significance of this method is that no prior information about critical temperature is needed:

$$\frac{M_S(T)}{dM_S(T)/dT} = \frac{T - T_c}{\beta}, \quad (4)$$

$$\frac{\chi_0^{-1}(T)}{d\chi_0^{-1}(T)/dT} = \frac{T - T_c}{\gamma}. \quad (5)$$

Equations (4) and (5) are linear functions of temperature with slopes $1/\beta$ and $1/\gamma$, respectively. Using this technique as shown in Fig. 4(b), the new obtained values of critical exponents are $\beta = 0.537 \pm 0.002$ with $T_c = 358.2 \pm 0.4$ K and $\gamma = 1.225 \pm 0.003$ with $T_c = 357.6 \pm 0.3$. It is worth mentioning that these values are in agreement with those obtained from a modified Arrott plot analysis. This shows that the values obtained are self-consistent and univocal.

Using the scaling hypothesis, magnetic equation of state in the asymptotic critical region can be expressed as [35]

$$M(H, \epsilon) = \epsilon^\beta f_\pm(H/\epsilon^{\beta+\gamma}), \quad (6)$$

where f_+ and f_- are regular functions for $T > T_c$ and $T < T_c$, respectively. Equation (6) implies that for true scaling relation and the right choice of critical exponents,

$M(H, \epsilon)\epsilon^{-\beta}$ vs $H\epsilon^{-(\beta+\gamma)}$ forms two independent curves for $T > T_c$ and $T < T_c$, respectively. In terms of renormalized magnetization as $m \equiv M(H, \epsilon)\epsilon^{-\beta}$ and renormalized $h \equiv \epsilon^{-(\beta+\gamma)}$, Eq.(6) can be written as

$$m = f_\pm h. \quad (7)$$

Based on Eq. (7), all the isothermal magnetizations are plotted and shown in Fig. 4(c), and one can clearly see that

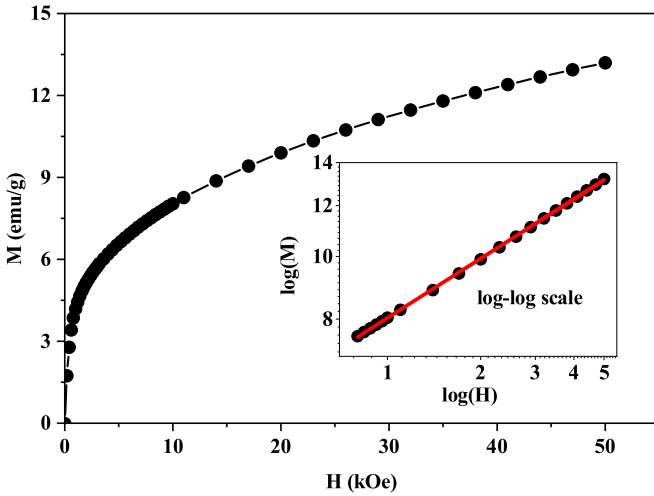


FIG. 5. Critical isotherm analysis at T_c . The inset shows the plot on \log_{10} - \log_{10} scale with a fitted solid line.

all the data fall on two independent branches for $T > T_c$ and $T < T_c$. The obedience of the scaling hypothesis reflects the reliability of critical exponents. Alternatively, the reliability is further verified with a more rigorous method by plotting m^2 vs h/m in Fig. 4(d), so that again all the isothermal magnetization data collapses onto two universal curves.

Using the above critical exponents the Curie temperature is determined to be 358 K. Figure 5 presents the isothermal magnetization at 358 K, with the same measurement on a \log_{10} - \log_{10} scale. According to Eq. (3), the \log_{10} - \log_{10} scale yields a straight line with slope $1/\delta$. The value obtained is $\delta = 3.261 \pm 0.002$. Alternatively, δ can be deduced using the Widom scaling relation [42], as follows:

$$\delta = 1 + \frac{\gamma}{\beta}. \quad (8)$$

Using the values of β and γ obtained from the KF method and modified Arrott plot, we deduced $\delta = (3.33 \pm 0.02)$ and $\delta = (3.33 \pm 0.07)$, respectively, which are much closed to the value obtained from critical isothermal analysis. Arrott-Noakes equation of state $(H/M)^{1/\gamma} = \epsilon + (M/M_1)^{1/\beta}$, where M_1 is constant and $\epsilon = (T - T_c)/T_c$ [43] is obeyed more strictly in the limit $T \approx T_c$. More universally, H/M vs M follows

$$(H/M)^{1/\gamma} = A' + B'M^{1/\beta}, \quad (9)$$

where A' and B' are temperature dependent coefficients. Thus taking all the critical exponents obtained using the KF method, all the isothermal magnetizations were reconstructed as $M^{1/\beta}$ vs $(H/M)^{1/\gamma}$, shown in Fig. 6(a). All the lines are very parallel to each other at high field region and the line at T_c passes through the origin. Figure 6(b) shows the plot between temperature dependent coefficients in Eq. (9) vs temperature. It can be clearly seen that A' passes through the origin at T_c and, in addition to this, the minima of B' is found to be located at T_c . All the results reveal that the critical exponents obtained by different methods in this work are consistent and reliable.

All the obtained critical exponents via different analytical techniques are listed in Table I with those of different theoretical models for comparison. It has been found that the

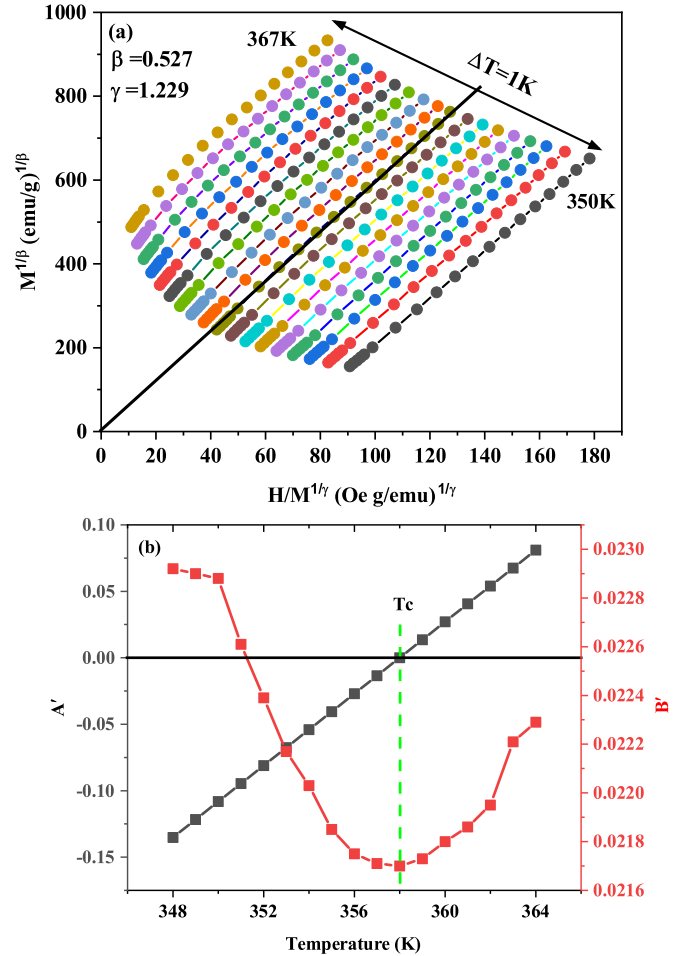
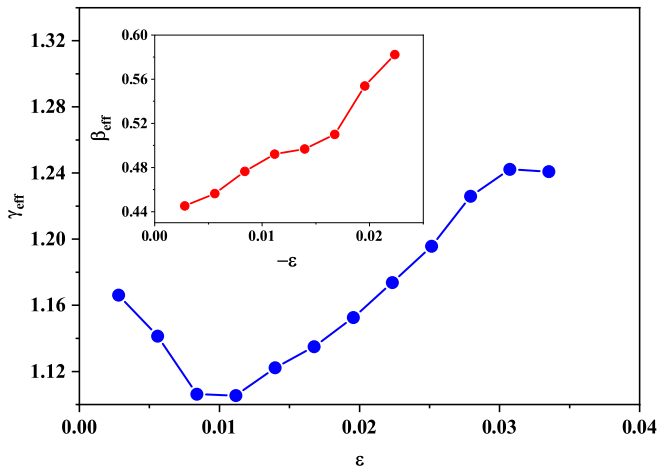


FIG. 6. (a) $(H/M)^{1/\gamma}$ vs $M^{1/\beta}$ with the critical exponents obtained by the KF method; (b) temperature dependence of modified coefficients A' and B' .

values of obtained critical exponents are close to that of the mean-field model, indicating the presence of long range magnetic ordering. However, deduced critical exponents slightly deviated from the theoretical values. It is important to know whether or not the obtained critical exponents belong to any of the universality class in the asymptotic region ($\epsilon \rightarrow 0$). For this purpose β_{eff} and γ_{eff} were obtained using the following

TABLE I. Comparison of critical exponents of Co_2TiSn with different theoretical models. MAP, modified Arrott plot; KF, Kouvel-Fisher method; CI, critical isotherm analysis.

Composition	References	Technique	β	γ	δ
Co_2TiSn	This work	MAP	0.527(3)	1.229(2)	3.33(2)
	This work	KF	0.537(2)	1.255(3)	3.33(7)
	This work	CI			3.261(2)
Ni	[37]	KF	0.391(10)	1.314(16)	4.39(2)
Co_2TiGe	[38]	KF	0.495(2)	1.324(4)	3.675
$\text{Gd}_{80}\text{Au}_{20}$	[39]	KF	0.44(2)	1.29(5)	3.96(3)
Mean field	[35]	Theory	0.5	1.0	3.0
3D Heisenberg	[33,40]	Theory	0.365	1.386	4.8
3D XY	[33,41]	Theory	0.345	1.316	4.81
3D Ising	[33,41]	Theory	0.325	1.24	4.82



- [1] C. Felser and G. H. Fecher, *Spintronics: From Materials to Devices* (Springer Science & Business Media, New York, 2013).
- [2] T. Graf, C. Felser, and S. S. Parkin, *Prog. Solid State Chem.* **39**, 1 (2011).
- [3] J. Kübler, G. H. Fecher, and C. Felser, *Phys. Rev. B* **76**, 024414 (2007).
- [4] H. C. Kandpal, G. H. Fecher, and C. Felser, *J. Phys. D: Appl. Phys.* **40**, 1507 (2007).
- [5] R. Sahoo, L. Wollmann, S. Selle, T. Höche, B. Ernst, A. Kalache, C. Shekhar, N. Kumar, S. Chadov, C. Felser, S. S. P. Parkin, and A. K. Nayak, *Adv. Mater.* **28**, 8499 (2016).
- [6] J. Kübler, A. R. William, and C. B. Sommers, *Phys. Rev. B* **28**, 1745 (1983).
- [7] I. Galanakis, P. H. Dederichs, and N. Papanikolaou, *Phys. Rev. B* **66**, 174429 (2002).
- [8] S. Parkin, X. Jiang, C. Kaiser, A. Panchula, K. Roche, and M. Samant, *Proc. IEEE* **91**, 661 (2003).
- [9] F. Pulizzi, *Spintronics* (Nature America, New York, 2012).
- [10] J. Barth, G. H. Fecher, B. Balke, T. Graf, A. Shkablo, A. Weidenkaff, P. Klaer, M. Kallmayer, H.-J. Elmers, H. Yoshikawa *et al.*, *Philos. Trans. R. Soc. A* **369**, 3588 (2011).
- [11] P. Klaer, M. Kallmayer, C. G. F. Blum, T. Graf, J. Barth, B. Balke, G. H. Fecher, C. Felser, and H. J. Elmers, *Phys. Rev. B* **80**, 144405 (2009).
- [12] S. J. Hashemifar, P. Kratzer, and M. Scheffler, *Phys. Rev. Lett.* **94**, 096402 (2005).
- [13] M. Jourdan, J. Minár, J. Braun, A. Kronenberg, S. Chadov, B. Balke, A. Gloskovskii, M. Kolbe, H. Elmers, G. Schönhense *et al.*, *Nat. Commun.* **5**, 3974 (2014).
- [14] R. Shan, H. Sukegawa, W. H. Wang, M. Kodzuka, T. Furubayashi, T. Ohkubo, S. Mitani, K. Inomata, and K. Hono, *Phys. Rev. Lett.* **102**, 246601 (2009).
- [15] S. Nakatsuji, N. Kiyohara, and T. Higo, *Nature (London)* **527**, 212 (2015).
- [16] J. Kübler and C. Felser, *EPL* **114**, 47005 (2016).
- [17] S. Gardelis, J. Androulakis, P. Migiakis, J. Giapintzakis, S. Clowes, Y. Bugoslavsky, W. Branford, Y. Miyoshi, and L. Cohen, *J. Appl. Phys.* **95**, 8063 (2004).
- [18] I. Shigeta, Y. Fujimoto, R. Ooka, Y. Nishisako, M. Tsujikawa, R. Y. Umetsu, A. Nomura, K. Yubuta, Y. Miura, T. Kanomata, M. Shirai, J. Gouchi, Y. Uwatoko, and M. Hiroi, *Phys. Rev. B* **97**, 104414 (2018).
- [19] J. Barth, G. H. Fecher, B. Balke, S. Ouardi, T. Graf, C. Felser, A. Shkablo, A. Weidenkaff, P. Klaer, H. J. Elmers, H. Yoshikawa, S. Ueda, and K. Kobayashi, *Phys. Rev. B* **81**, 064404 (2010).
- [20] S. Majumdar, M. K. Chattopadhyay, V. K. Sharma, K. J. S. Sokhey, S. B. Roy, and P. Chaddah, *Phys. Rev. B* **72**, 012417 (2005).
- [21] M. Meinert, J. Schmalhorst, H. Wulfmeier, G. Reiss, E. Arenholz, T. Graf, and C. Felser, *Phys. Rev. B* **83**, 064412 (2011).
- [22] G. Chang, S.-Y. Xu, H. Zheng, B. Singh, C.-H. Hsu, G. Bian, N. Alidoust, I. Belopolski, D. S. Sanchez, S. Zhang *et al.*, *Sci. Rep.* **6**, 38839 (2016).
- [23] B. Ernst, R. Sahoo, Y. Sun, J. Nayak, L. MÜchler, A. K. Nayak, N. Kumar, J. Gayles, A. Markou, G. H. Fecher, and C. Felser, *Phys. Rev. B* **100**, 054445 (2019).
- [24] J. Fan, L. Ling, B. Hong, L. Zhang, L. Pi, and Y. Zhang, *Phys. Rev. B* **81**, 144426 (2010).
- [25] K. Ghosh, C. J. Lobb, R. L. Greene, S. G. Karabashev, D. A. Shulyatev, A. A. Arsenov, and Y. Mukovskii, *Phys. Rev. Lett.* **81**, 4740 (1998).
- [26] L. Zhang, J. Fan, L. Li, R. Li, L. Ling, Z. Qu, W. Tong, S. Tan, and Y. Zhang, *EPL* **91**, 57001 (2010).
- [27] A. K. Pramanik and A. Banerjee, *Phys. Rev. B* **79**, 214426 (2009).
- [28] B. Deka, R. Das, and A. Srinivasan, *J. Magn. Magn. Mater.* **347**, 101 (2013).
- [29] Y. Miura, K. Nagao, and M. Shirai, *Phys. Rev. B* **69**, 144413 (2004).
- [30] Y. Fujita, K. Endo, M. Terada, and R. Kimura, *J. Phys. Chem. Solids* **33**, 1443 (1972).
- [31] L. Bainsla and K. Suresh, *Curr. Appl. Phys.* **16**, 68 (2016).
- [32] A. Arrott, *Phys. Rev.* **108**, 1394 (1957).
- [33] B. Banerjee, *Phys. Lett.* **12**, 16 (1964).
- [34] M. E. Fisher, *Rep. Prog. Phys.* **31**, 418 (1968).
- [35] H. E. Stanley, *Phase Transitions and Critical Phenomena* (Clarendon Press, Oxford, 1971).
- [36] L. P. Kadanoff, *Phys. Phys. Fiz.* **2**, 263 (1966).
- [37] M. Seeger, S. N. Kaul, H. Kronmüller, and R. Reisser, *Phys. Rev. B* **51**, 12585 (1995).
- [38] S. Roy, N. Khan, R. Singha, A. Pariari, and P. Mandal, *Phys. Rev. B* **99**, 214414 (2019).
- [39] S. J. Poon and J. Durand, *Phys. Rev. B* **16**, 316 (1977).
- [40] M. Camprostrini, M. Hasenbusch, A. Pelissetto, P. Rossi, and E. Vicari, *Phys. Rev. B* **65**, 144520 (2002).
- [41] J. C. Le Guillou and J. Zinn-Justin, *Phys. Rev. B* **21**, 3976 (1980).
- [42] B. Widom, *J. Chem. Phys.* **43**, 3892 (1965).
- [43] A. Arrott and J. E. Noakes, *Phys. Rev. Lett.* **19**, 786 (1967).
- [44] A. Perumal, V. Srinivas, V. V. Rao, and R. A. Dunlap, *Phys. Rev. Lett.* **91**, 137202 (2003).
- [45] L. P. Kadanoff, W. Götze, D. Hamblen, R. Hecht, E. A. S. Lewis, V. V. Palciauskas, M. Rayl, J. Swift, D. Aspnes, and J. Kane, *Rev. Mod. Phys.* **39**, 395 (1967).
- [46] J. Mira, J. Rivas, M. Vázquez, J. M. García-Beneytez, J. Arcas, R. D. Sánchez, and M. A. Señaris-Rodríguez, *Phys. Rev. B* **59**, 123 (1999).
- [47] M. Hickey, A. Husmann, S. Holmes, and G. Jones, *J. Phys.: Condens. Matter* **18**, 2897 (2006).